

Modelling Fluid Inflow Equalisation using Inflow Control Devices on Horizontal Compartmentalised Oil Wells: Case Study of Niger Delta Oilfield

Hassan Babidi Yahya, Nnaemeka Princewill Ohia, Ifeanyi Michael Onyejekwe, Ugochukwu Ilozurike Duru, Stanley Tooohukwu Ekwueme, Angela Nkechi Nwachukwu

Department of Petroleum Engineering, Federal University of Technology, Owerri, Nigeria

Received November 27, 2023; Accepted March 14, 2024

Abstract

This study focuses on the modelling wellbore compartmentalization techniques for downhole flow control in both homogeneous and heterogeneous oil reservoirs. The objective was to achieve fluid inflow equalization to address variable productivity effects (VPE) in heterogeneous multilayered reservoirs and to ensure flow uniformity across horizontal intervals in homogeneous reservoirs, mitigating the heel-to-toe effect (THE) caused by frictional pressure drop in horizontal well completions. The compartmentalization along the wellbore was achieved using swellable packers, ensuring each well compartment had uniform productivity before equalization. Inflow equalization across compartments was accomplished using inflow control devices (ICDs). Analytical models for ICDs were developed based on fundamental fluid flow equations, including Darcy's and Bernoulli's equations. Simulation of the developed model was conducted using MATLAB 2014Rb. Three simulation cases were explored: Case 1 studied variable pressure effects in homogeneous reservoirs where pressure and permeability influenced inflow inequality; Case 2 examined variable pressure effects considering pressure, permeability, and skin as factors for inflow variation; Case 3 simulated inflow equalization in horizontal homogeneous reservoirs to counteract the heel-to-toe effects. The results demonstrated successful equalization in all cases: Case 1 achieved a target well production rate of 7500 stb/d; Case 2 resulted in a total target well inflow rate of 6250 stb/d; Case 3 achieved a composite well inflow rate of 15000 stb/d. Implementation of variable ICDs in the horizontal well segment prevented early water/gas breakthrough due to THE, enhancing well longevity and recovery efficiency, thereby improving total well recovery.

Keywords: *Compartmentalisation; ICDs; Inflow equalisation; Swellable packers; Variable production; Darcy Law.*

1. Introduction

Advancements in drilling and completions technology have transformed the extraction of oil from complex petroleum reservoirs, making it more cost-effective [1]. These innovations have facilitated the drilling of highly deviated wells, ensuring maximum reservoir contact, even in previously challenging reservoirs [2]. Maximum-reservoir-contact (MRC) wells offer several advantages over conventional wells, such as higher productivity, enhanced sweep efficiency, and increased well drainage area. In particular, horizontal wells have demonstrated significant efficiency in enhancing oil recovery compared to vertical wells [3-4]. They increase the contact area between the wellbore and the reservoir, leading to improved oil drainage and high production rates at lower pressure drawdown [5-6].

However, in heterogeneous reservoirs, challenges arise due to non-uniform sanding conditions, water coning along the wellbore, and the heel-toe effect, where frictional pressure losses increase with well length [7]. This non-uniformity distorts the inflow profile, causing the heel part of the well to produce more fluid than the toe. This issue has been addressed through

various studies [8-9]. Furthermore, the specific inflow rate varies due to factors like pressure losses and reservoir heterogeneity, causing imbalances in fluid inflow. This imbalance adversely affects oil sweep efficiency and overall recovery [10]. Heel-to-toe effect in horizontal wells leads to an early breakthrough of water or gas in the heel section, causing operational challenges and impacting the ultimate recovery from the reservoir [11-12].

Uneven fluid inflow rates in wells often result from reservoir heterogeneities, which refer to variations in properties such as permeability, porosity, thickness, and fluid pressures within the reservoir volume [4]. To address this challenge, reservoirs are compartmentalized into sections with similar properties, making them easier to model [13]. Each compartment shares common hydraulic parameters, making it essential for effective reservoir management. Compartmentalization is typically based on criteria such as fluid flow rate or reservoir pressure, ensuring equal flow rates or pressures within each compartment [14-15].

Innovative downhole flow control devices, like inflow control devices (ICDs), have emerged as advanced completion technology to manage these complexities. ICDs play a vital role in regulating individual well performance and overall reservoir behaviour, particularly in mitigating breakthrough challenges [16]. These devices are integrated into well completions to achieve a uniform inflow profile, even in the presence of reservoir heterogeneities. By equalizing inflow along the wellbore's lateral length, ICDs ensure that the entire well contributes evenly to total production [17-18]. Additionally, they help prevent annular flow issues that can lead to plugging and screen erosion. ICDs achieve this balance by creating a controlled pressure drop at the sandface through a choking mechanism, ensuring consistent inflow rates at specified flow rates.

Several studies have focused on Inflow Control Device (ICD) configuration in horizontal wells. Birchenko *et al.* [2] developed an analytical model for ICD completed horizontal wells in homogeneous reservoirs, emphasizing the importance of considering production uniformity and reduced output when deciding ICD parameters. Gurses and Vasper [19] explored conflicting optimization objectives and identified three strategies based on segmenting and ICD configuration differences. They utilized the Simplex method and artificial neural network algorithms for optimization. Dowlatabad [20] investigated cumulative oil production, determining optimal ICD configuration and segmenting positions in horizontal wells through the level set method. This study demonstrated that segmented ICD completion significantly enhances inflow profiles and recovery rates.

Wang *et al.* [21] demonstrated that Inflow Control Devices (ICDs) effectively reduce water production and enhance oil recovery in heterogeneous reservoirs with bottom water by equalizing pressure drop and altering flow direction. Zhang *et al.* [22] developed a multi-objective optimization method for configuring ICDs in horizontal wells, outperforming single-objective optimization and openhole completion methods. Eltaher *et al.* [23] investigated Autonomous Flow Control Completions (AFCC) using dynamic reservoir simulation, offering a reliable approach to evaluate AFCC technology's benefits and select optimal completions.

2. Fluid flow modelling from reservoir to wellbore through ICDs

For the wellbore fitted with ICDs, the reservoir fluid flows from the formation via the annulus to the ICDs. The fluid continues its flow from the ICDs which offers some pressure drop to the tubing (or pipe), after which it flows to the surface. In modelling, we divide the reservoir-wellbore system into three comprising the reservoir (sandface), the ICD and the inner tubing (or pipe). Various equations account for the fluid flow and pressure drops in various phases from the sand face (reservoir to the ICD and to the tubing).

2.1. Modelling fluid flow through the reservoir

The flow of fluid at the sand face within the porous media or reservoir section follows the Darcy fluid flow equation for porous media. Among the various parameters influencing fluid movement in the reservoir, the most crucial one is the Inflow Performance Relationship (IPR) [24]. This relationship establishes a connection between the pressure drop across the formation and the resulting flowrate. Darcy's equations for porous media are utilized to characterize fluid flow under different conditions, including steady state, pseudo-steady state, and transient

state, involving both single-phase and multiphase fluids. The IPR exhibits variations based on factors such as well architecture (vertical or horizontal wells), the stage of reservoir depletion (above or below the bubble point pressure), and the specific fluid phases being produced or injected [25].

The well's IPR can be defined by productivity index J, the productivity index for horizontal well for single and multiphase flow into the wellbore are given in equation 1 and 2 respectively

$$J = \frac{b\sqrt{k_{ox}k_{oz}}}{141.2\beta_o\mu_o \left[\ln \left(\frac{h\sqrt{\frac{k_{ox}}{k_{oz}}}}{r_w \left(h\sqrt{\frac{k_{ox}}{k_{oz}}} \right)} + \frac{\pi x_p}{h\sqrt{\frac{k_{ox}}{k_{oz}}}} - 1.224 + S + S_R \right) \right]} \quad (1)$$

$$j = \frac{b\sqrt{k_x k_z}}{141.2\beta_o\mu_o \left[\ln \left(\frac{h\sqrt{\frac{k_x}{k_z}}}{r_w \left(h\sqrt{\frac{k_x}{k_z}} \right)} + \frac{\pi x_p}{h\sqrt{\frac{k_x}{k_z}}} - 1.224 + S + S_R \right) \right]} \left(\frac{k_{ro}}{\beta_o\mu_o} \right) \quad (2)$$

where: b = extension of the drainage volume in the y direction, here b represents the direction of the wellbore (ft); k_x = absolute permeability in the x direction (md); k_y = absolute permeability in the y direction (md); k_{ox} = effective permeability to oil in the x direction (md); k_{oy} = effective permeability to oil in the y direction (md); A = drainage area of the segment; oh , (ft²); S_{Rskin} resulting from partial penetration.

2.2. Modelling fluid flow across the ICD

When fluid flows through Inflow Control Device (ICD) nozzles, there are pressure drops due to friction and acceleration. Given the short flow path through the nozzles, the frictional pressure drop can be considered negligible, only the pressure drop resulting from the velocity loss as the fluid passes through the ICD nozzles will be considered. The flow through an ICD nozzle can be represented by Bernoulli equation for fluid flow through a constriction. The pressure drop ICD equation for multiphase of gas, oil/water is given in equation 3

$$\delta P_{ICD} = \frac{8C_u\rho_{mix}q_{ICD}^2(1-\beta^4)}{C_{(Re)}^2\varepsilon^2\pi^2d_{no}^4} \quad (3)$$

$$\rho_{mix} = \alpha_o\rho_o + \alpha_g\rho_g + \alpha_w\rho_w \quad (4)$$

$$\beta = \frac{d_{no}}{D_{cr}} \quad (5)$$

$$D_{cr} = \sqrt{d_{chout}^2 - d_{chin}^2} \quad (6)$$

where: δP_{ICD} = pressure drop across the icd nozzle, psi; ρ_{mix} = density of mixture f oil, gas and water (lb/cuft); q_{ICD} = flowrate of fluid in the icd, stb/d; C_u = conversion factor which is 0.0002159; $C_{(Re)}$ = nozzle discharge coefficient based on reynolds number (dimensionless); d_{no} = diameter of the nozzle-type icd, ft; ε = gas expansibility factor (dimensionless); β = ratio of nozzle/orifice diameter to upstream pipe diameter (dimensionless); $\rho_{o,g,w}$ =, density of oil, gas and water phases at in-situ conditions; $\alpha_{o,g,w}$ = volume fraction of oil, gas and water phases at in-situ conditions; d_{cr} = clearance diameter of the icd restriction chamber ahead of nozzles; d_{chout} = chamber outer diameter, ft; d_{chin} = chamber inner diameter, ft.

The nozzle coefficient $C_{(Re)}$ for nozzle-type ICD can be determined using equation 7

$$C_{(Re)} = 0.99 - 0.2262\beta^{4.1} - (0.00175\beta^2 - 0.0033\beta^{4.15}) \left(\frac{10^6}{Re_D} \right)^{1.15} \quad (7)$$

The Reynolds number in oil field units is given in equation 8

$$Re_D = \frac{92.24 q \cdot SG}{\mu D_{cr}} \quad (8)$$

where: Re_D = Reynolds number of the flow in the region upstream of the icd nozzle; q = fluid flowrate, stb/d; sg = specific gravity of fluid; μ = viscosity of the fluid, cP.

For single phase flow of oil the ICD pressure drop equation approximates to

$$\delta P_{ICD} = \frac{8C_u\rho_o q_{ICD}^2(1-\beta^4)}{C_{(Re)}^2\pi^2d_{no}^4} \quad (9)$$

where: ρ_o = density of the oil, stb/d.

2.3. Modelling fluid flow in the wellbore

The wellbore flow consists of acceleration pressure, friction pressure drop, and gravity pressure drop [22]. However, since a horizontal wellbore is considered, the acceleration and gravity pressure drop are negligible. Thus, the frictional pressure drop in the horizontal wellbore is given by Darcy-Weisbach given in equation 10 as

$$\frac{dP}{dL} = (11.5 * 10^{-6}) \frac{fQ^2(SG)}{D^5} \quad (10)$$

where: D is the pipe inside diameter; f is the Darcy-Weisbach friction factor; L is the length of the pipe; Q is the fluid flow rate b/d; SG is the specific gravity of the fluid relative to water; dp/dL is the pressure drop in psi/ft.

When $Re_D \leq 2000$, the flow is of laminar regime; $2000 < Re_D < 4000$, the flow is in transitional phase; $Re_D > 4000$, the flow is turbulent.

Equation 11 and equation 12 gives the friction factor for laminar and turbulent flow respectively

$$f = \frac{64}{Re_D} \quad (11)$$

$$\frac{1}{\sqrt{f}} = -2 \log_{10} \left(\frac{e}{3.7D} + \frac{2.51}{Re_D \sqrt{f}} \right) \quad (12)$$

where: f = Darcy friction factor, dimensionless; D = the pipe internal diameter, inches; e = absolute pipe roughness, inches; R = The Reynolds number, dimensionless.

Equation 12 is the Colebrook-White equation which is an implicit equation since the friction factor f appears on both sides of the equation. The Swamee-Jain equation which is an acceptable approximation of the Colebrook-White equation is given in equation 13. The Swamee-Jain equation is a good approximation of the Colebrook-white equation.

$$f = \frac{0.25}{[\log_{10}(e/3.7D + 5.74/R^{0.9})]^2} \quad (13)$$

2.4. Modelling of fluid flow through wellbore and completions with and without ICDs

To account for the fluid flow in the wellbore, completions and tubing both for the case with and without ICD, proper modelling methodology is conducted. The assumptions for this modelling approach are following:

- i. The fluid is single phase oil;
- ii. The reservoir and wellbore length are segmented in the direction of the wellbore with each segmented having distinct hydraulic parameters;
- iii. The edges of the reservoir are modelled as no-flow boundary;
- iv. The reservoir and fluid properties (the permeability, pressure, viscosity, etc.) within a segment are constant;
- v. The flow is steady state;
- vi. The well is horizontal.
- vii. In homogenous reservoir fluid inflow variation is only caused by heel to toe effect occasioned by pressure drop along the wellbore length.
- viii. In heterogeneous reservoir, inflow variation could be caused by/or combination of reservoir heterogeneity and heel-to-toe effect (HTE).

2.4.1. Modelling of the coupled fluid inflow without ICD

To identify the fluid influx in the original case without ICD, the reservoir is coupled to the wellbore. Since the wellbore is divided into various segments along the reservoir-wellbore length, the fluid influx from the reservoir into each of the tubing segment is represented by the equation given in equation 14

$$q_{in}(i) = PI_s(i) [\bar{P}_r(i) - P_{wbf}(i)] \quad (14)$$

where: q_{in} = Fluid influx rate for the segment; PI_s = Segment productivity index; \bar{P}_r = Reservoir pressure for the segment; P_{wbf} = wellbore flowing pressure for the segment; i = segment number. Figure 1 illustrates the physical model representation of modelling of the coupled fluid flow without ICD.

The fluid flowing from each wellbore segment node towards the topmost node is the sum of the fluid influx from the reservoir and the fluid flowing from the bottom segment. The

exception is the first node from the bottom (toe) of the well where the tubing flow rate is equivalent to the fluid influx rate:

$$\sum_{i=1}^n q_s(i) = q_{in}(i) + \sum_{i=1}^{i-1} q_s(i) \tag{15}$$

where: q_s = wellbore segment flowrate; q_{in} = total flowrate at the topmost section of the well (heel); n = number of segments.

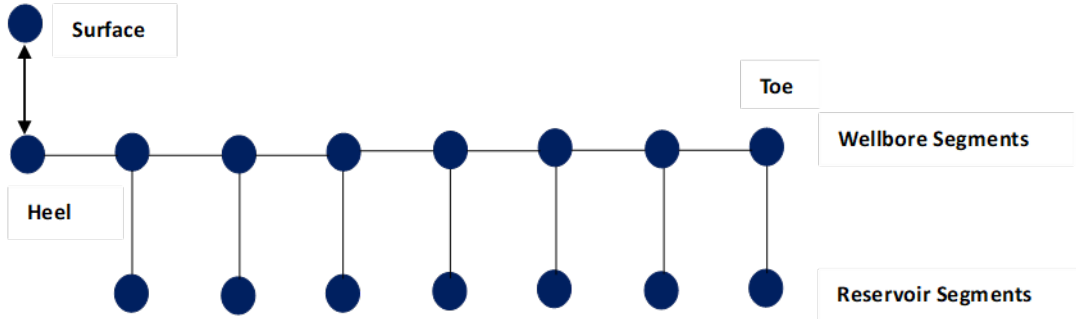


Figure 1. Coupled reservoir /wellbore fluid flow mode.

2.4.2. Modelling of fluid inflow with ICD restriction and sizing

ICD provides additional pressure drop to the flow into the tubing. ICD of various sizes and diameter are used to control the pressure drop. The fluid flow when ICD is used is a function of the pressure drop through the ICD and is given in equation 16

$$q_{ICD}(i) = P_{ICD}(i) [\bar{P}_r(i) - P_{wbf}(i) - \delta P_{ICD}(i)] \tag{16}$$

where: P_{ICD} = productivity index of the reservoir segment with length equivalent to the ICD, δP_{ICD} = pressure drop across the ICD, q_{ICD} = fluid inflow into the ICD

The pressure drop across a nozzle-type ICD is given in equation 3. Plugging equation 3 into equation 16 and making q_{in} the subject of formula yields

$$q_{ICD}(i) = \frac{-1 + \sqrt{1 + \frac{32C_u}{\pi^2} \left[\frac{P_{ICD}^2 \rho_{mix} (1 - \beta^4)}{C_{(Re)}^2 \epsilon^2 d_{no}^4} \right] (i) [\bar{P}_r(i) - P_{wbf}(i)]}}{\frac{16C_u P_{ICD} \rho_{mix} (i)}{\pi^2 C_{(Re)}^2 \epsilon^2 d_{no}^4}} \tag{17}$$

For single phase oil flow, equation 17 becomes

$$q_{ICD}(i) = \frac{-1 + \sqrt{1 + \frac{32C_u}{\pi^2} \left[\frac{P_{ICD}^2 \rho_o (1 - \beta^4)}{C_{(Re)}^2 d_{no}^4} \right] (i) [\bar{P}_r(i) - P_{wbf}(i)]}}{\frac{16C_u P_{ICD} \rho_o (i)}{\pi^2 C_{(Re)}^2 d_{no}^4}} \tag{18}$$

The physical model illustrating the coupled fluid flow across an ICD is shown in Figure 2.

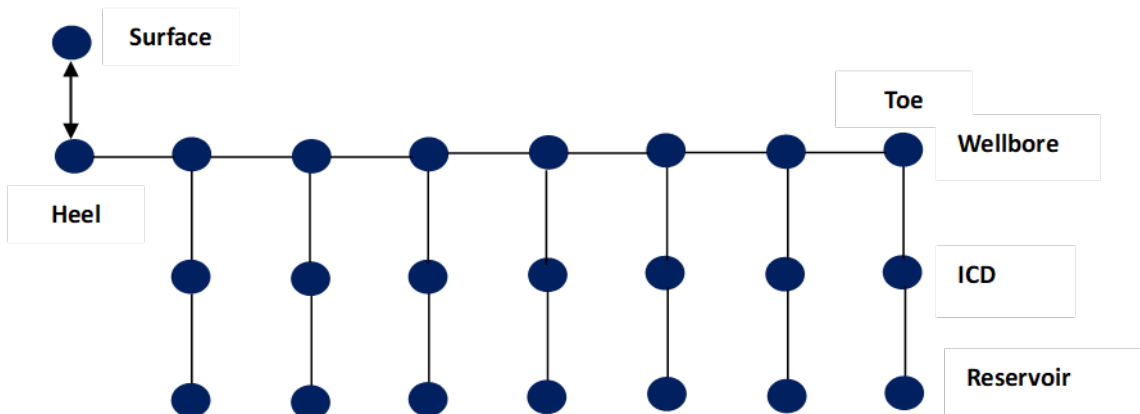


Figure 2. Reservoir/ICD/wellbore fluid flow model.

2.4.3. Modelling with ICD indicating the well segments

This model is represented by depicting the various ICDs and flow in each segment. The ICD is modelled such that the ICDs in each segment are identical due to similar properties. The equations for this are similar to equations 16, 17 and 18 under section 2.4.1. The physical for the coupled flow modelling with ICD indicating the segments is given in Figure 3.

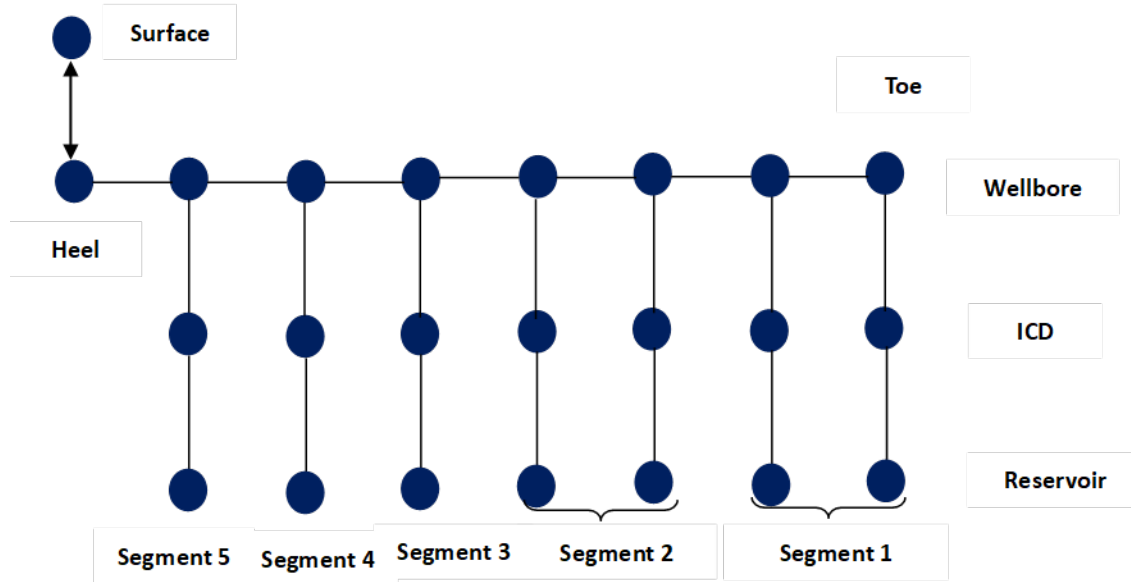


Figure 3. Reservoir/ICD/wellbore fluid flow model showing the compartmentalized segments.

2.4.4. ICD completion design

The fluid flow through any two ICDs located in a well should either be equivalent or equalized to the "optimum" point. An "equivalent" inflow (or outflow) rate per tubular joint (q_{eq}) can be calculated by dividing the target well flow rate by the number of standard tubular (i.e., ICD) joints which can be installed across the producing segment

$$q_{eq} = \frac{q_t}{N_j} \quad (19)$$

where: q_{eq} = equal segment influx rate; N_j = number of completion joints.

Nevertheless, it is crucial to emphasize that achieving the optimal equalization flow rate requires careful consideration of the completion length. In this case, the segment influx rates might not be identical initially. However, equalization is attained as the fluid travels along the completion length, influenced by pressure drop effects throughout the entire completion. For optimum equalization to be achieved the flowrate in the highest productivity segment must be equal to or approximately equal to the flow rate in the lowest productivity segment which is taken as the reference segment.

$$q_{ICDH} \cong q_{ICDR} \quad (20)$$

The flow rate from a section of the well equivalent in length to the size of an ICD joint is governed by the productivity of that section

$$PI_{ICD} = J_s L_{ICD} \quad (21)$$

where J_s = Specific productivity index; L_{ICD} = length of ICD joint.

The target wellbore flowing pressure is given in equation 22

$$P_{wf} = P_{rL} - \delta P_{PGSAS} - \left(\frac{q_{eq}}{PI_{ICDL}} \right) \quad (22)$$

where: P_{wf} = wellbore flowing pressure (for initial use); P_{rL} = reservoir pressure in the low permeability segment; δP_{PGSAS} = pressure drop across a gravel pack or sas; PI_{ICDL} = productivity index of the across icd length in the low permeability segment, psi.

The flowrate in the low permeability area is chosen so that it equalizes the flowrate in the high permeability area. In the reference low permeability segment, no ICD is used, but in the subsequent higher permeability segments ICDs are used to lower the influx rate

To achieve equal flowrate, the influx rate for the high productivity segment and the low productivity segment are equated together. This is given in equation 23

$$q_{ICDH} = q_{ICDL} \tag{23}$$

$$PI_{ICDH}(i)[\bar{P}_{rH}(i) - P_{wbfH}(i) - \delta P_{ICD}(i)] = PI_{ICDL}(i)[\bar{P}_{rL}(i) - P_{wbfL}(i) - \delta P_{PGSAS}(i)] \tag{24}$$

Making δP_{ICD} the subject of the formula yields 25

$$\delta P_{ICD} = \bar{P}_{rH} - \frac{PI_{ICDL}}{PI_{ICDH}} [\bar{P}_{rL} - P_{wbfL} - \delta P_{PGSAS}] - P_{wbf} \tag{25}$$

If the components causing the productivity variation can be identified, then the δP_{ICD} can be rewritten to address these components individually. If permeability is the only component causing the variation, then it means that other components like reservoir pressure, skin, wellbore and reservoir radii, reservoir thickness are the same; the equation becomes:

$$\delta P_{ICD} = \bar{P}_{rH} - \frac{k_L}{k_H} [\bar{P}_{rL} - P_{wbfL} - \delta P_{PGSAS}] - P_{wbf} \tag{26}$$

If the wellbore pressure drop is negligible then

$$\delta P_{ICD} = \frac{q_t}{N_{ICDj}L_{ICD}} \left(\frac{h_L}{PI_L} - \frac{h_H}{PI_H} \right) + \delta P_{PGSAS} \tag{27}$$

This can be further expressed as

$$\delta P_{ICD} = \frac{q_{s-eq}}{j_{sL}} - \frac{q_{s-eq}}{j_{sL}} + \delta P_{PGSAS} \tag{28}$$

where q_{s-eq} is the equalized specific flowrate.

Haven determined δP_{ICD} , the size of the nozzle ICD can be determined from the equation

$$\delta P_{ICD} = \frac{8C_u \rho_{mix} q_{ICD}^2 (1-\beta^4)}{C_{(Re)}^2 \varepsilon^2 \pi^2 d_{no}^4} \tag{29}$$

Making nozzle diameter the subject of the formula gives

$$d_{no} = \sqrt[4]{\frac{8C_u \rho_{mix} q_{ICD}^2 (1-\beta^4)}{\delta P_{ICD} C_{(Re)}^2 \varepsilon^2 \pi^2}} \tag{30}$$

When oil is the only phase, the nozzle size equation is given by

$$d_{no} = \sqrt[4]{\frac{8C_u \rho_o q_{ICD}^2 (1-\beta^4)}{\delta P_{ICD} C_{(Re)}^2 \pi^2}} \tag{31}$$

The discharge coefficient due to Reynolds number can be replaced with the discharge coefficient due to valve position, Cd

$$d_{no} = \sqrt[4]{\frac{8C_u \rho_o q_{ICD}^2 (1-\beta^4)}{\delta P_{ICD} C_d^2 \pi^2}} \tag{32}$$

3. Case study

ABX is an oilfield in the Niger Delta region of Nigeria. ABX comprises reservoirs ABX1 ABX2 and ABX3 predominantly sandstone formation with strong bottom water. ABX field is prone to serious water production due to high watercut occasioned by variable inflow rates. The differences in inflow rates were due to reservoir heterogeneities which affects the ultimate recovery from the field. To solve the problem of water production and increase ultimate recovery, it was resolved to compartmentalise the wellbore and install ICDs to offer back pressure to high inflow segments such that constant well inflow would be achieved for each well across the wellbores. For this to be achieved, three cases were considered to investigate the variations in reservoir conditions in the field. Case 1 and case 2 investigated the variable fluid inflow caused by reservoir heterogeneities. The ICDs that would be installed at compartmentalised wellbore segments are intended to achieve wellbore inflow equalisation. Case 3 considered the heel-to-toe effect in horizontal well by installing ICD that address the frictional pressure drops along the horizontal interval The heel-to-effect was caused by frictional pressure variation along the horizontal wellbore length that makes the heel section to have more drawdown and hence more fluid influx than the toe section.

For Case 1, productivity variation was solely influenced by permeability, reservoir thickness, and segment drainage area, with all other reservoir properties remaining constant. For Case 2, variations in pressure, permeability, thickness, and skin were observed across different segments. Case 3 involved simulating Heel-to-Toe Effects (HTE) in the horizontal wellbore section of a homogeneous reservoir.

Tables 1, 2, and 3 provide the wellbore, reservoir, and fluid data for the respective cases. The wellbore was divided into five segments in each case, with uniform reservoir properties within each segment. Swellable packers were employed to compartmentalize the wellbore. Equalization was achieved by referencing the segment with the lowest productivity. The goal was to maintain a consistent fluid influx rate across the lateral sections by strategically placing Inflow Control Devices (ICDs) with higher pressure drop across completion joints of segments with higher productivity index. Conversely, ICDs with lower pressure drop were placed across segments with lower productivity index.

Table 1. Reservoir and PVT properties for case 1.

Parameters	Segment 1	Segment 2	Segment 3	Segment 4	Segment 5
Density, lbm/cuft	53.7	53.7	53.7	53.7	53.7
Layer drainage area, acres	40	50	30	45	35
Reservoir pressure, psi	3000	3000	3000	3000	3000
Reservoir temperature, °F	220	220	220	220	220
Viscosity, cP	1.2	1.2	1.2	1.2	1.2
API	33	33	33	33	33
Oil fv _f	1.23	1.23	1.23	1.23	1.23
Layer permeability, md	500	650	750	800	850
Layer thickness, ft	138.6	145.6	140.4	125.2	135.8
Layer skin factor, S	5	5	5	5	5
Pipe size (ID), inch	5.5	5.5	5.5	5.5	5.5
Pipe roughness, inch	0.0018	0.0018	0.0018	0.0018	0.0018

Table 2. Reservoir and PVT Properties for Case 2

Parameters	Lateral 1	Lateral 2	Compartment 3	Compartment 4	Compartment 5
Density, lbm/cuft	53.7	53.7	53.7	53.7	53.7
Layer drainage area, acres	40	50	30	45	35
Reservoir pressure, psi	2980	3000	3100	3050	3020
Reservoir temperature, °F	220	220	220	220	220
Viscosity, cP	1.2	1.2	1.2	1.2	1.2
API	33	33	33	33	33
Oil fv _f	1.23	1.23	1.23	1.23	1.23
Layer Permeability, md	500	650	750	800	850
Layer Thickness, ft	138.6	145.6	140.4	125.2	135.8
Layer Skin Factor	5	3.5	4	4.5	5
Pipe size (ID), inch	5.5	5.5	5.5	5.5	5.5
Pipe roughness, inch	0.0018	0.0018	0.0018	0.0018	0.0018

Table 3. Reservoir and Well Parameters for Case 3

Parameters	Value	Parameters	Value
Density lbm/cuft	53.7	Layer skin factor	5
Layer drainage area, acres	230	Wellbore radius, ft	0.354
Reservoir pressure, psi	3000	Length of Well, ft	800
Reservoir Temperature, °F	220	ICD length per joint, ft	40
Viscosity, cP	1.2	Tubing roughness, inch	0.0018
API	33	Total well depth, ft	33135
Oil fv _f	1.23	Horizontal anisotropy	1
Layer Permeability, mD	800	Vertical anisotropy	0.2
Layer thickness, ft	138.6		

The target of the fluid inflow equalization was to calculate the sizes ICDs that could ensure uniform fluid influx across the sand-face to achieve the desired total well inflow rate. To accomplish this, a specific approach was adopted: low-strength ICDs were installed in the low productivity segments, while high-strength ICDs were placed in the high productivity segments.

Two equalization techniques were explored for this purpose. In the first approach, a Self-Adjusting Sleeve (SAS) completion was employed in the lowest productivity segment while other segments were fitted with ICDs of various sizes based on the calculated pressure drops they needed to accommodate. The second approach involved installing the lowest strength ICD in the lowest productivity segment instead of using SAS completion. This modification aimed to minimize potential increases in inflow that might occur with SAS usage.

In both approaches, the total target flowrate encompassed the combined flowrates from all segments. The equalization scheme referenced the lowest productivity segment, requiring adjustments in the productivity of other segments to align with the flowrate calculated for the lowest productivity segment.

4. Results

4.1. Results for Case 1 simulation

4.1.1. Segment productivity index

The well productivity before ICD placement was first determined by plotting IPR curves of each segment. The IPR curves of each segment enabled the determination of the productivity index from each segment and the composite (total) well productivity. Figure 4 gives the well productivity for the different segments and the composite well productivity before ICD placement.

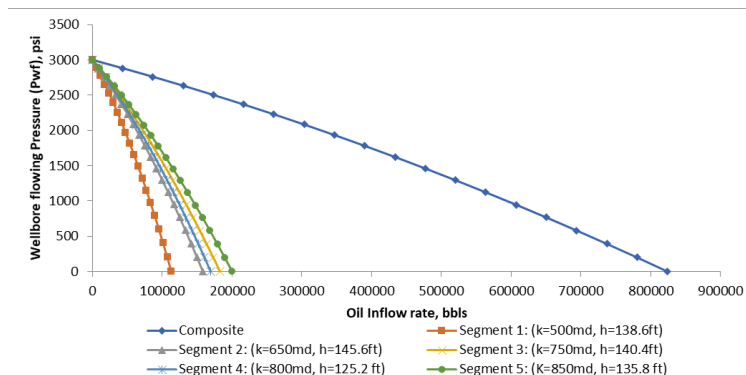


Figure 4. IPR for case 1 showing productivity potentials for various segments and the composite (total) well performance.

The productivity index of each segment is illustrated in Figure 4. It can be seen from Figure 4 that segment 1 has the lowest PI of 53.3 stb/d/psi, while segment 5 has the highest PI which is 87.8 stb/d/psi.

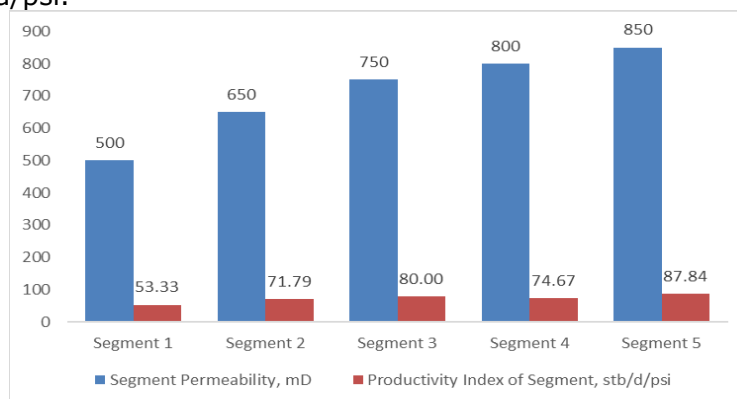


Figure 5. Productivity index and permeability of each segment for case 1.

The observed highest PI in segment 5 is due to the fact that it has the highest segment permeability.

4.1.2. Segment ICD sizing

In the first approach, a Self-Adjusting Sleeve (SAS) was utilized in the lowest productivity segment, while Inflow Control Devices (ICDs) were employed in the remaining segments or layers. The target total well inflow rate for each segment was set at 6250 stb/d. Consequently, all five segments were modelled to achieve an inflow rate of 1250 stb/d. The lowest productivity segment, equipped with the SAS completion, produced 1250 stb/d. To equalize the inflow rates, ICDs of various sizes were strategically placed in the other segments, individually adjusting their inflow rates to 1250 stb/d. The placement of ICDs was determined based on the required pressure drops necessary for back pressure to achieve inflow equalization.

Table 4. Nozzle sizes for productivity equalization across segments (with SAS at the lowest productivity segment).

Segment Number	Productivity index of segment (stb/d/psi)	Pressure drop across ICD (psi)	ICD nozzle diameter (mm)
1	53.33	0	SAS
2	71.79	6.03	17.3
3	80.00	7.81	16.2
4	74.67	6.70	16.8
5	87.84	9.21	15.5

Table 4 provides information on the pressure drop across each segment and the corresponding Inflow Control Device (ICD) sizes necessary to achieve fluid equalization across the segments, addressing the variable production effects (VPE) resulting from the heterogeneous reservoir system. Analysis of Table 4 reveals that segment 5 exhibits the highest productivity index (87.84 stb/d/psi), necessitating the highest ICD pressure drop of 9.21 psi. This translates to an ICD nozzle diameter size of 15.5 mm per ICD joint. In segment 4, an ICD imposing a pressure drop of 6.7 psi required an ICD nozzle diameter size of 16.8 mm per ICD joint. Similarly, for another segment 4 scenario, an ICD with a pressure drop of 7.81 psi necessitated an ICD nozzle diameter size of 16.2 mm per ICD joint. In yet another segment 4 case, an ICD generating a pressure drop of 6.03 psi resulted in an ICD nozzle diameter size of 17.3 mm per ICD joint.

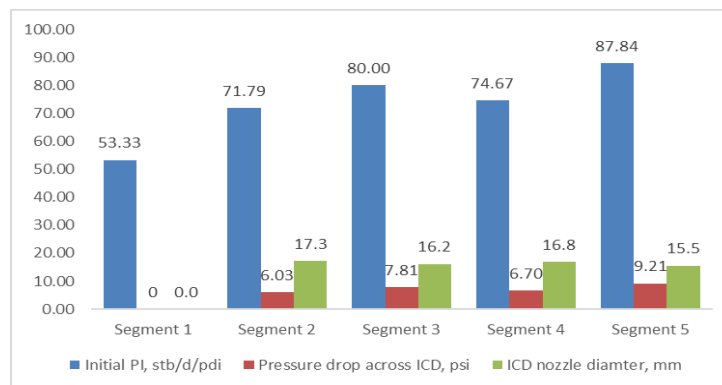


Figure 6. ICD Pressure drop and ICD nozzle diameter for each segment (with SAS of 0 psi in lowest PI segment).

From Figure 6, notice that for segment 1, the pressure drop is zero since no ICD was placed there, but the segment was modelled using SAS completion with negligible pressure drop

The second approach aimed to prevent annular flow by replacing the SAS with ICDs of very low pressure drop in the lowest productivity segment, which is segment 1. By selecting ICDs with minimal pressure drop, resistance to fluid flow in this segment was significantly reduced. A specific ICD offering a pressure drop of 9.3 psi was chosen to replace SAS in segment 1. Consequently, segment 1's productivity index and wellbore flowing pressure served as the

reference points for equalizing fluid influx rates across the entire wellbore length. Figure 7 illustrates the ICD data for each segment, including the ICD size, pressure drop, and PI.

From Figure 7, it becomes evident that introducing the ICD in segment 1, rather than using SAS completion, altered the required pressure drops for the ICDs in each segment.

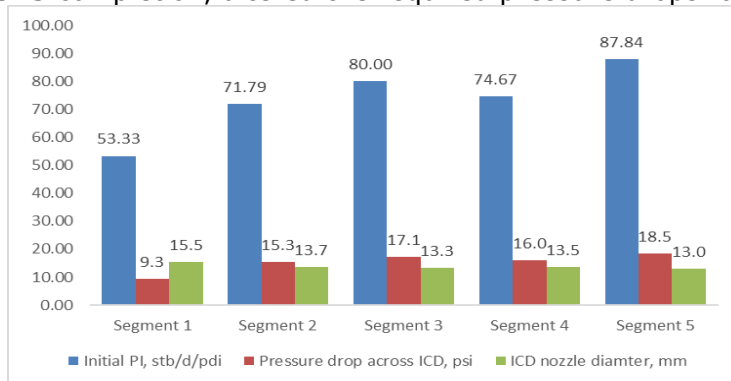


Figure 7. ICD Pressure drop and ICD nozzle diameter for each segment by incorporating ICD in lowest PI segment.

Similarly, in segment 4, an ICD generating a pressure drop of 17.1 psi resulted in an ICD nozzle diameter size of 13.5 mm per ICD joint. Lastly, in segment 5, an ICD imposing a pressure drop of 18.5 psi needed an ICD nozzle diameter size of 13 mm per ICD joint. Notice that for segment 1, the pressure drop is not zero as in Figure 6 since an ICD of 9.3 psi pressure loss was installed. The equalized IPR plot is given in Figure 8.

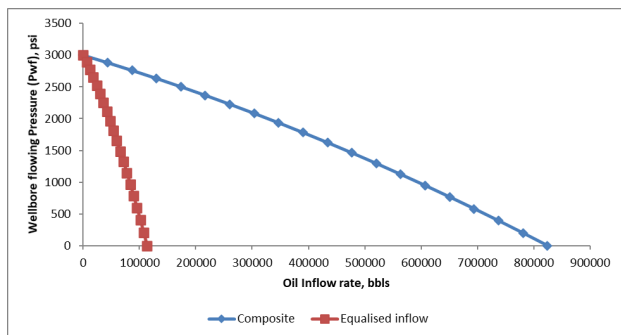


Figure 8. Equalized IPR plot for case 1 after ICD deployment across segments.

with the anticipated total well influx rate of 6250 stb/d, as indicated by the composite IPR curve at the same wellbore flowing pressure of 2976.56 psi.

Figure 9 shows that at a wellbore flowing pressure of 2976.56 psi, all the segments gave a fluid influx rate of 1250 stb/d. This translates to a composite (total) production rate of 6250 stb/d.

Figure 10 shows the fluid influx with and without ICDs for each wellbore segment indicating the flowrate when the segments were produced with a wellbore flowing pressure of 2976.56 psi without ICDs before inflow equalization and the current equalized inflow rate due to ICD placement.

It can be seen from Figure 11 that before inflow equalization, the segments all had varied fluid inflow rates across each segment which were 1250 stb/d, 1683 stb/d, 1875 stb/d, 1750 stb/d and 2059 stb/d for segment 1, segment 2, segment 3, segment 4 and segment 5 respectively. However, a uniform equalised fluid inflow rate of 1500 stb/d was achieved using ICDs of various sizes placed across each segment.

Consequently, the ICD sizes needed for fluid inflow equalization varied across the segments. Due to the implementation of the 9.3 psi ICD in segment 1, an ICD size of 15.5 mm was used. In segment 2, an ICD imposing a pressure drop of 15.3 psi required an ICD nozzle diameter size of 13.7 mm per ICD joint. In segment 3, an ICD with a pressure drop of 17.1 psi required an ICD nozzle diameter size of 13.3mm per ICD joint.

In Figure 8, a consistent inflow is observed across all segments, depicted by the unchanging IPR curve. The red line in Figure 8 represents uniform well productivity across all segments, while the blue line signifies the composite IPR curve representing the combined well influx rate from all five segments. Figure 8 also illustrates a constant wellbore flowing pressure maintained for all segments. At a wellbore flowing pressure of 2976.78 psi, each lateral yields 1500 stb/d, aligning

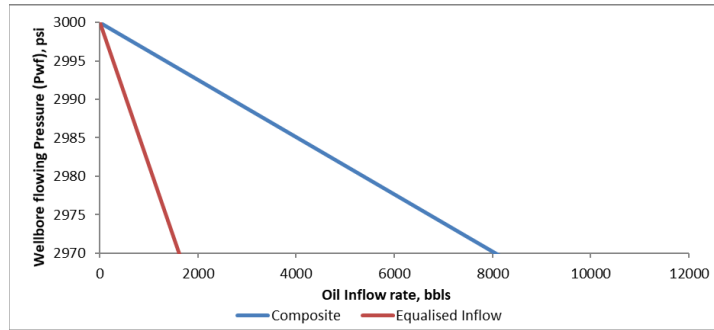


Figure 9. Equalized contribution from all segments due to ICD placement across segments for case 1.

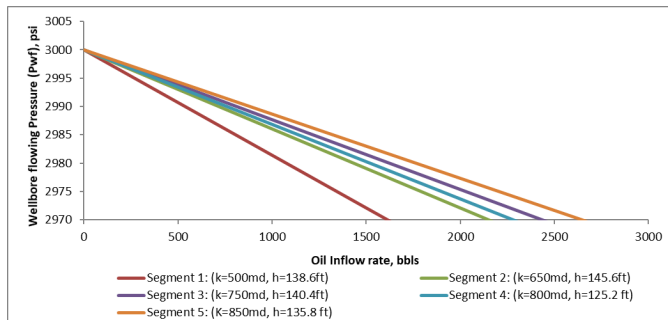


Figure 10. Fluid inflow from various segments at $p_{wf}=2976.56$ psi before equalization for case 1

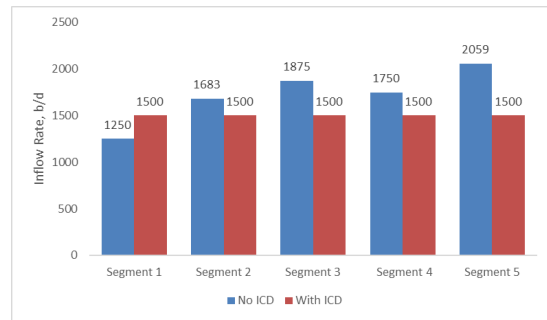


Figure 11. Fluid inflow across segments before and after equalization for case 1.

4.2. Results for Case 2 simulation

4.2.1. Segment productivity index

First the inflow performance curve for each segment and the composite system were plotted. The composite curve shows the cumulative productivity index in the reservoir from all the segments. Figure 12 gives the IPR plot for case 2. From Figure 12 it can be seen that in terms of increasing absolute open flow potential (AOF), the segments are as follows: segment 1, Segment 2, segment 4, Segment 5 and Segment 3. Segment 3 was observed to have the largest AOF while segment 1 had the lowest AOF. However, the AOF alone is not a good representation of the productivity potentials of each segment. The productivity index of each segment are given in Figure 13.

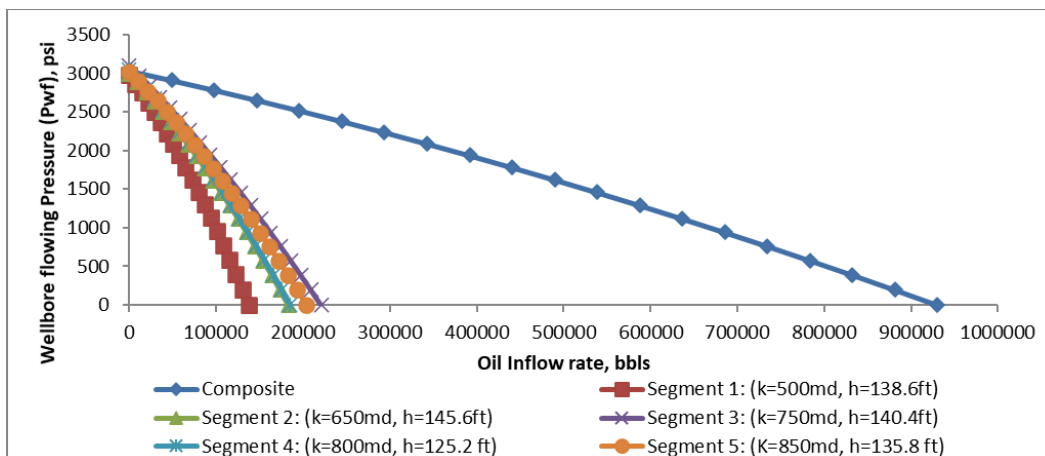


Figure 12. IPR for case 2 showing productivity potentials for various segments and the composite (total) well performance.

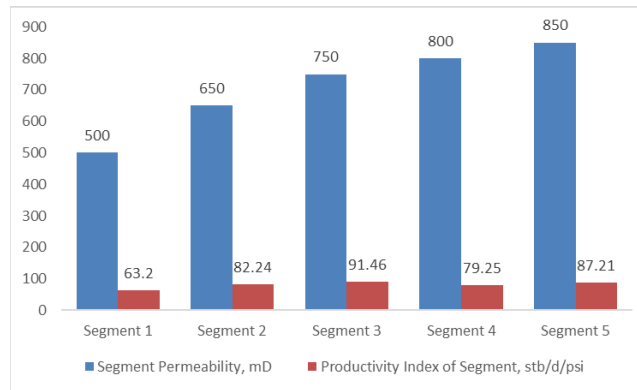


Figure 13. Productivity index and permeability of each segment for case 2.

The productivity index of each segment and the corresponding permeability are shown in Figure 13. It can be seen from Figure 13 that segment 1 has the least PI of 63.2 stb/d/psi, while segment 3 has the highest PI which is 91.46 stb/d/psi. This is due to facts that it has relatively permeability, segment pressure, segment thickness and skin.

4.2.2. ICD sizing for various segments for Case 2

The target total flowrate from the well is 7500 stb/d. Two approaches were considered. In the first approach, SAS completion with negligible pressure drop was placed across the lowest productivity segment (segment 1) and ICDs of variable sizes are placed across other segments respectively. The target equalised well influx flowrate across each segment is 1500 stb/d. A SAS completion with a negligible pressure drop would have required a wellbore flowing pressure of 3015 psi to yield 7500 stb/d (i.e., using the composite IPR). The ICD sizes that would be deployed across each segment to achieve a constant fluid influx rate of 1250 stb/d across the segments were calculated. The ICD sizes and pressure drops calculated for each segment are shown in Figure 14.

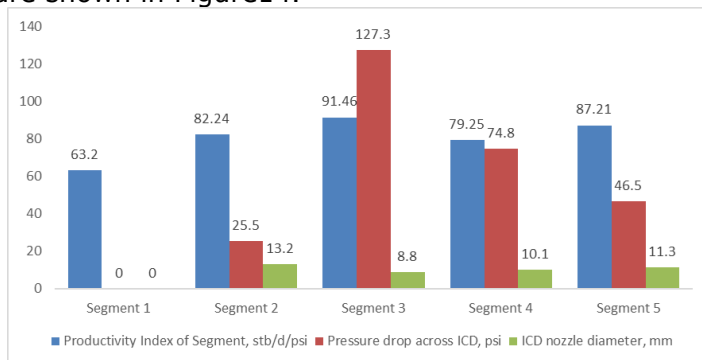


Figure 14. ICD Pressure drop and ICD nozzle diameter for each segment for case 2

Figure 14 shows the pressure drop across segments and the corresponding ICDs sizes required to achieve fluid equalization, addressing the variable production effects (VPE) caused by the heterogeneous reservoir system. Notably, segment 1 shows zero pressure drop since no ICD was placed there; instead, it was modelled using SAS completion with negligible pressure drop. Figure 14 demonstrates a trend where smaller ICD sizes (indicating higher

pressure drops) are installed in segments with higher productivity. For instance, segment 3, with the highest productivity index of 91.46 stb/day/psi, required an ICD imposing a pressure drop of 127.3 psi at the completion joint to reduce fluid influx from that segment to the desired 1500 stb/d. This required an ICD diameter of 8.8 mm. Similarly, for segment 4, an ICD with a pressure drop of 74.68 psi was needed, requiring an ICD diameter of 10.1 mm to achieve fluid inflow equalization. In segment 5, an ICD that would create a pressure drop of 46.5 psi was required, corresponding to an ICD diameter of 11.3 mm. Segment 2 required an ICD diameter of 13.2 mm to achieve fluid influx equalization, given a calculated pressure drop of 25.5 psi in that segment.

The second approach aimed to prevent annular flow by replacing SAS with an ICD of very low pressure drop in the lowest productivity segment (segment 1). The selected ICD had

minimal pressure drop, minimizing resistance to fluid flow in this segment. An ICD with a pressure drop of 9.3 psi was chosen to replace SAS at segment 1. Consequently, segment 1's productivity and wellbore flowing pressure served as the reference points for equalizing fluid influx rates across the entire completion length. Figure 15 shows the ICD sizes used for each segment.

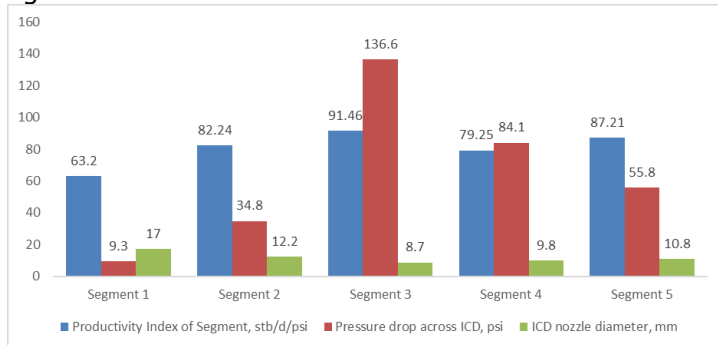


Figure 15. ICD Pressure drop and ICD nozzle diameter for each segment.

From Figure 15, it can be observed that the inclusion of ICD at segment 1 instead of SAS completion changes the required ICD pressure drop for each segment and consequently the ICD sizes require for fluid inflow equalization across the segments. The ICD size required for segment 1 with a calculated ICD pressure drop of 9.3 psi is 17 mm diameter. The ICD size required for segment 2 with a calculated ICD pressure drop of 34.8 psi

is 12.2 mm diameter ICD. The ICD required for segment 3 with a calculated ICD pressure drop of 136.6 psi is 8.7 mm diameter ICD. The ICD size required for segment 4 with a calculated ICD pressure drop of 84.1 psi is 9.8 mm. the ICD size required for segment 5 with a calculated ICD pressure drop of 55.5 psi is 10.8 mm ICD diameter.

Whichever approach used; the ICD deployment achieved equalization of fluid inflow across the segments. This enables flow monitoring and checks against excessive water production (rising watercut).The equalized IPR plot for case 2 simulation is shown in Figure16.

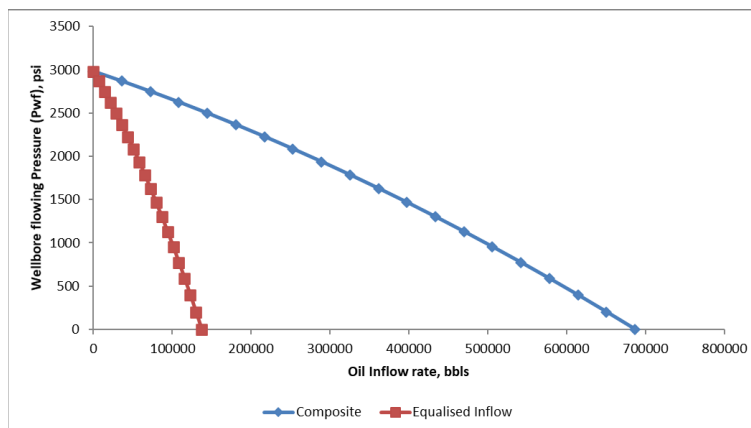


Figure 16. Equalized IPR plot for case 2 after ICD deployment across segments.

From Figure16, it can be seen that all the segments have equal inflow as indicated by a constant IPR curve. The blue line in Figure15 represents the equal well productivity for all the segments while the green line is the composite IPR curve representing the total well influx rate coming from all the five segments summed together.

Figure 17 shows the wellbore the constant wellbore flowing pressure for which all the segments are produced. Figure 17 also shows that at 2956.3 psi (wellbore flowing pressure), the various laterals yield 1500 stb/d. As expected, this corresponded to a total well influx rate of 7500 stb/d as indicated by the composite IPR curve at the same wellbore flowing pressure of 2956.3.

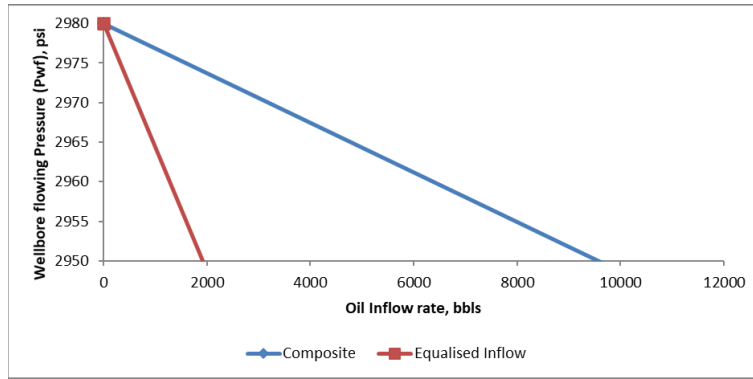


Figure 17. Equalized contribution from all segments due to ICD placement across segments for case 2.

Figure 17 shows that at a wellbore flowing pressure of 2956.3 psi, all the laterals gave a fluid influx rate of 1500 stb/d. This translates to a composite (total) production rate of 7500 stb/d. It is important to consider the fluid influx rate with and without ICD at the wellbore flowing pressure of 2956.3 psi since it was used across the segments. This would give information about the extent of the equalization achieved through the placement of the ICDs across the segments.

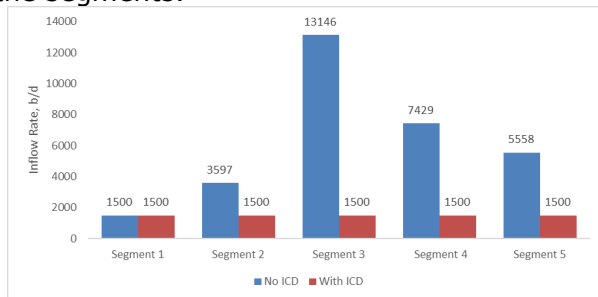


Figure 18. Fluid inflow across segments before and after equalization for case 2.

Figure 18 shows the wellbore segments inflow rates with and without ICDs indicating the flowrate that would have been achieved if the segments were produced with a wellbore flowing pressure of 2956.3 psi without inflow equalization and the current equalized inflow rate due to ICD placement.

It can be seen that without equalization, the segments all have varied fluid inflow rates. The inflow rates across the segments are 1500 stb/d, 3596.5 stb/d, 13146.3 stb/d,

7428.7stb/d and 5558.1 stb/d for segment 1, segment 2, segment 3, segment 4 and segment 5 respectively. A constant fluid inflow rate of 1500 stb/d was achieved after equalization using ICDs of various sizes placed across segments.

4.3. Results for Case 3 simulation

In Case 3, a horizontal wellbore was drilled through a homogeneous reservoir. In this configuration, the productivity index remains consistent as long as each section of the wellbore is subjected to the same drawdown pressure. However, due to frictional pressure, the flowing wellbore pressure varies along the horizontal length of the wellbore, causing the heel section to experience greater drawdown than the toe section under identical reservoir conditions. This discrepancy in inflow between the heel and toe sections is influenced by the well's length and the friction within the pipe walls, leading to high water-cuts.

To address this issue, ICDs were strategically placed along the entire length of the wellbore to achieve equalization of fluid inflow. The horizontal wellbore, measuring 800 ft in length, was divided into 20 segments, each of length 40 ft. The goal was to achieve a total well flowrate of 15000 stb/d, with a target flowrate of 750 stb/d for each segment. Initially, it was observed that the heel and toe sections were producing 1000 stb/d and 750 stb/d, respectively, before the equalization process began. The Inflow Performance Relationship (IPR) of the well prior to the installation of ICDs is depicted in Figure 19.

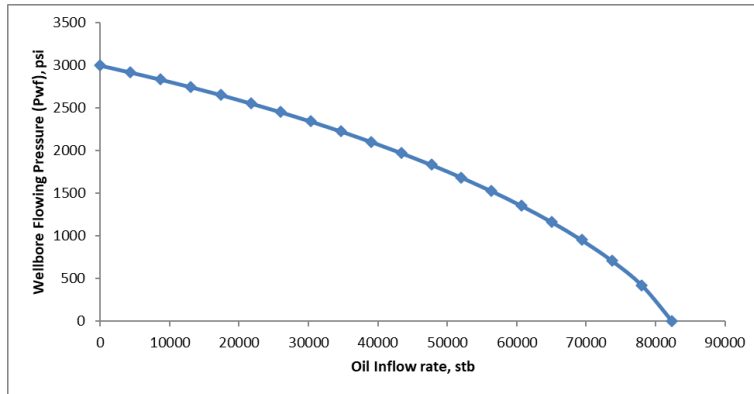


Figure 19. Productivity plot for the total well performance for case 3.

Figure 19 illustrates the productivity plot for the well, indicating the contributing segments along the wellbore length. The well's productivity index is 55.56 stb/d/psi. If a Self-Adjusting Sleeve (SAS) completion with negligible pressure drop were used, a wellbore flowing pressure of 2730 psi would be required to achieve the target total well inflow rate.

However, the objective is to design Inflow Control Devices (ICDs) to be installed across the wellbore segments, equalizing inflow to 750 stb/d per segment, summing up to 15000 stb/d from the well. The calculated wellbore flowing pressure at the toe was 2986.5 psi, while at the heel section, before the deployment of ICDs, it was calculated to be 2981.1 psi. The wellbore flowing pressure profile due to friction before the installation of ICD is shown in Figure 20.

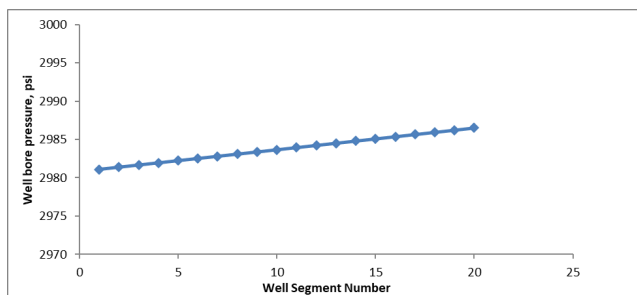


Figure 20. Wellbore pressure variation across wellbore segments from heel to toe.

In Figure 20, it is evident that before the installation of Inflow Control Devices (ICDs), the flowing wellbore pressure varies across the different segments of the well, from heel to toe. There is a progressive increase in wellbore flowing pressure along the horizontal wellbore, indicating higher drawdown at the heel section due to reduced wellbore flowing pressure. This pressure profile explains the higher productivity observed at the heel section and the lower productivity at the toe section.

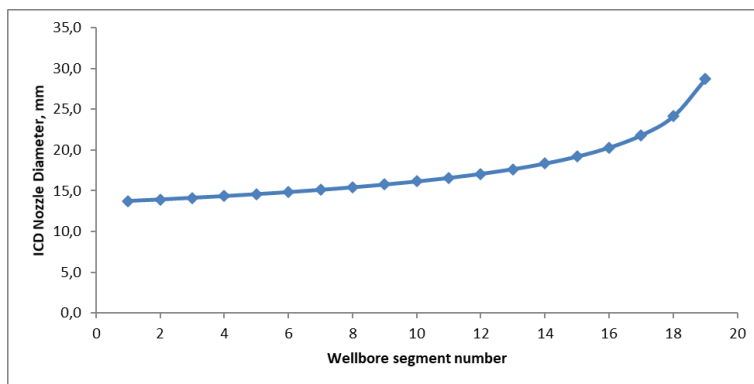


Figure 21. ICD nozzle sizes for wellbore segments.

Figure 21 gives the ICD sizes design for the inflow equalization across the horizontal wellbore length. Note that segment 21 was completed with SAS offering zero psi pressure drop.

It can be seen from Figure 20 that the ICD size increases with the wellbore segment number from the heel to the toe of the well. Smaller ICD sizes are required to for higher pressure drop. Pressure drops increases from the toe to the heel section.

Smaller ICDs restricts more flow and are required at the heel section of the wellbore. A SAS completion of negligible pressure drop was installed at the toe section. The flowrate before and after the equalization process is depicted in Figure 22.

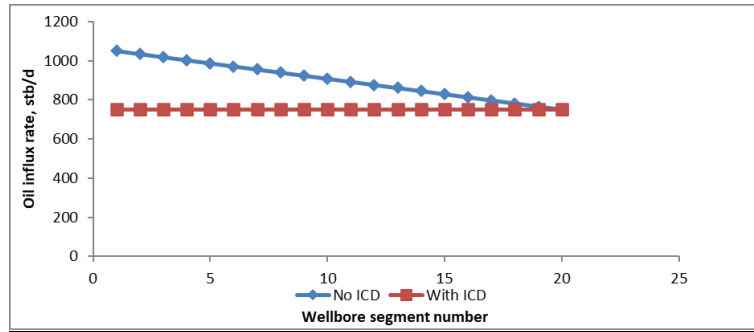


Figure 22. Oil influx rate before and after equalization using variable ICDs.

Figure 22 gives the oil influx rate before and after equalization using variable ICD sizes. It is evident that the installation of variable ICDs achieved full equalization across the wellbore segments. An equal influx rate of 750 stb/d was achieved across the wellbore segments.

5. Conclusion

Extensive modelling of wellbore-reservoir interactions was undertaken for both homogeneous and heterogeneous reservoirs. The modelling was performed to identify segments exhibiting variable productivity effects (VPE) in a multi-segmented reservoir and to analyze the variations in frictional pressure drop causing heel-toe effects (THE) in a homogeneous reservoir. The reservoir was divided into uniform productivity segments, each characterized by identical reservoir parameters. To achieve precise compartmentalization and enable separate modelling of each segment, swellable packers were employed in the wellbore-reservoir system. This approach enabled the installation of ICDs to achieve complete equalization of the inflow rates across the various compartmentalized segments. The mathematical models developed for inflow equalization, both in homogeneous and heterogeneous reservoir systems, proved to be effective, ensuring complete equalization across the segmented sections through the strategic use of variable Inflow Control Devices (ICDs). Notably, the study demonstrated the successful installation of different-sized nozzle-type ICDs in each segment of the multi-segmented heterogeneous reservoir system. This approach led to the realization of target well production rates, thereby optimizing reservoir performance. In case 1, a balanced inflow rate of 1500 stb/d was achieved for each wellbore segment, leading to a targeted well production rate of 7500 stb/d. In case 2, the equalized inflow rate in each wellbore segment reached was 1250 stb/d, resulting in an overall targeted well inflow rate of 6250 stb/d.

Furthermore, in the case of homogeneous horizontal wellbores, the study showcased the strategic placement of ICDs along the wellbore length. This placement effectively equalized the inflow rates by mitigating variations caused by frictional pressure drop from heel-to-toe effects. The outcome was a composite well inflow rate that met the desired production targets, underscoring the importance of precise ICD placement in optimizing reservoir production. For this case, an equalized wellbore segment inflow rate of 750 stb/d was achieved, contributing to an overall composite well inflow rate of 15,000 stb/d.

A key achievement of the research was the prevention of early water breakthrough, which was a major of the field visible in the high watercuts, through the implementation of variable ICDs. This preventive measure significantly improved the well's longevity and recovery efficiency, ultimately enhancing the overall reservoir recovery.

References

- [1] Nnakaihe SE, Duru UI, Ohia NP, Obah BO, Nwabia FN. Enhancing the Effectiveness of Vertical Water Injection Wells with Inflow Control Devices (ICDs): Design, Simulation and Economics, 2017
- [2] Vasily M. Analytical Modeling of Wells with inflow Control Devices (Doctoral dissertation, Ph. D. Dissertation, Heriot-Watt University). 2010.
- [3] Mode AW, Adepehin EJ, Anyiam OA. Petrophysical effects of clay heterogeneity on reservoirs' properties: case study of "Brown Field" Niger Delta, Nigeria. Niger Assoc Pet Explor Bull., 2013; 25(1):61-9.
- [4] Sallam MA, El-Banbi AH. Analysis of multi-layered commingled and compartmentalized gas reservoirs. Journal of Petroleum Exploration and Production Technology, 2018; 8:1573-86.

- [5] Agoha CC, Opara AI, Okeke OC, Okereke CN, Akaolisa CC, Onwubuariri CN, Omenikolo IA, Agbakwuru CB. Reservoirs Stability Evaluation through Analysis of Rock Mechanical Parameters and Stresses in "Beta" Field, Offshore Niger Delta, Nigeria. *Pet Coal*, 2023; 1:65(3).
- [6] Muradov K, Eltaher E, Davies D. Reservoir simulator-friendly model of fluid-selective, down-hole flow control completion performance. *Journal of Petroleum Science and Engineering*, 2018; 164:140-54.
- [7] Eltaher EM. Modelling and applications of autonomous flow control devices (Doctoral dissertation, Heriot-Watt University). 2017.
- [8] Birchenko VM, Bejan AI, Usnich AV, Davies DR. Application of inflow control devices to heterogeneous reservoirs. *Journal of Petroleum Science and Engineering*, 2011; 78(2):534-41.
- [9] James EJ, Hossain MM. Evaluation of factors influencing the effectiveness of passive and autonomous inflow control devices. In *SPE Asia Pacific Oil and Gas Conference and Exhibition 2017*; (p. D012S036R062). SPE.
- [10] Al-Khelaiwi FT, Birchenko VM, Konopczynski MR, Davies DR. Advanced wells: a comprehensive approach to the selection between passive and active inflow-control completions. *SPE Production & Operations*, 2010; 25(03):305-26.
- [11] Smith PE, Young D, Shahreyar N, Lauritzen JE, Awang MZ. The Bulkhead Principle—Delaying Water Cut and Improving Horizontal Well Productivity through Compartmentalization Using Short Swellable Packers. In *SPE Asia Pacific Oil and Gas Conf. and Exhib. 2011*; (SPE-147877).
- [12] Jovanov I. Performance of autonomous inflow control systems (Master's thesis, University of Stavanger, Norway). 2016.
- [13] Sallam MA, El-Banbi AH. Analysis of multi-layered commingled and compartmentalized gas reservoirs. *Journal of Petroleum Exploration and Production Technology*, 2018; 8:1573-86.
- [14] Go J, Smalley PC, Muggeridge A. Appraisal of reservoir compartmentalization using fluid mixing time-scales: Horn Mountain Field, Gulf of Mexico. *Petroleum Geoscience*, 2012; 18(3):305-14.
- [15] Irving AD, Chavanne E, Faure V, Buffet P, Barber E. An uncertainty modelling workflow for structurally compartmentalized reservoirs. Geological Society, London, Special Publications. 2010; 347(1):283-99.
- [16] Izadi H, Leung JY, Roostaei M, Mahmoudi M, Stevenson J, Tuttle A, Sutton C, Mirzavand R, Fattahpour V. A practical workflow to design inflow control devices in SAGD projects to increase production and lower fresh water usage. *Fuel*, 2024; 356:129454.
- [17] Acencios L, Garcia W, Huaranga L, Guerrero X, Camelo S, Gurses S, Williams B. Increased Oil and Reduced Water Production Using Cyclonic AICDs with Tracer Monitoring Applications in Peru's Bretaña Norte Field. In *SPE Annual Technical Conference and Exhibition? 2023*; (p. D021S022R003). SPE.
- [18] Hamd-Allah SM. Analyzing of Production Data Using Combination of empirical Methods and Advanced Analytical Techniques. *Petroleum & Coal*, 2023; 65(4): 1023-1032.
- [19] Gurses S, Vasper A. Optimized modeling workflows for designing passive flow control devices in horizontal wells. In *SPE Reservoir Characterisation and Simulation Conference and Exhibition? 2013*; (pp. SPE-166052). SPE.
- [20] Dowlatabad MM. Novel Integrated Approach Simultaneously Optimising AFI Locations Plus Number and (A) ICD Sizes. In *SPE Europec featured at EAGE Conference and Exhibition? 2015*; (pp. SPE-174309). SPE.
- [21] Wang J, Liu H, Liu Y, Jiao Y, Wu J, Kang A. Mechanism and sensitivity analysis of an inflow control devices (ICDs) for reducing water production in heterogeneous oil reservoir with bottom water. *Journal of Petroleum Science and Engineering*, 2016; 146:971-82.
- [22] Zhang R, Zhang Z, Li Z, Jia Z, Yang B, Zhang J, Zhang C, Zhang G, Yu S. A multi-objective optimization method of inflow control device configuration. *Journal of Petroleum Science and Engineering*. 2021; 205:108855.
- [23] Eltaher E, Muradov K, Davies D, Grassick P. Autonomous flow control device modelling and completion optimisation. *Journal of Petroleum Science and Engineering*. 2019; 177:995-1009.
- [24] Al-Khelaiwi FT. A comprehensive approach to the design of advanced well completions (Doctoral dissertation, Heriot-Watt University). 2013.
- [25] Irani M, Bashtani F, Kantzas A. Control of gas cresting/coning in horizontal wells with tubing-deployed inflow control devices. *Fuel*, 2021; 293:120328.

To whom correspondence should be addressed: Stanley Toochukwu Ekwueme, Department of Petroleum Engineering, Federal University of Technology, Owerri, Nigeria, E-mail: stanleyekwueme@yahoo.com